



Benjamin M. Statler College of
Engineering and Mineral Resources
Department of Chemical and Biomedical Engineering

DISSERTATION RESEARCH PROPOSAL

STRATEGIES FOR PROCESS SYSTEMS MAPPING AND CONTROL BASED ON OPERABILITY ANALYSIS

Research Advisor: Dr. Fernando V. Lima
Ph.D. Student: Victor Alves

Morgantown, June 28, 2023

Keywords: operability analysis, gaussian processes, automatic differentiation, control structure selection

Copyright 2023 Victor Alves

Project Summary: This research aims to develop strategies for process systems engineering (PSE) mapping using models, emerging tools and algorithms motivated by process operability research. Such strategies will be employed to ensure simultaneous design and control of large-scale industrial systems. The emerging tools and techniques in this research range from supervised machine learning-based (ML-based) operability mapping, to the use of automatic differentiation (AD) for implicit mapping, and the development of a systematic mapping approach for control structure selection using operability analysis. The preliminary results show that the proposed approach for the ML-based mapping has the potential to tackle the curse of dimensionality when addressing large-scale systems while keeping accuracy within 0.3% for the worst-case scenario when compared to classic nonlinear programming-based (NLP) mapping techniques. In addition, the reductions in computational time are up to four orders of magnitude. For the novel AD-based mapping, the accuracy is also guaranteed to be within around 0.02%, while the computational time is reduced from 19.2 times to 111% faster depending on the implementation of the compared nonlinear programming formulation. Lastly, the developed approach for control structure selection using operability analysis is capable of ranking posed control structures according to their operability characteristics using the operability index as a metric.

Intellectual Merit: Thus far, the developed operability algorithms either recur to NLP solutions which are computationally expensive or to linearizing the underlying mapping task at the expense of losing accuracy. In addition, the combinatorics properties inherent to the control structure selection problem are yet to be addressed using operability analysis. Therefore, the existing gaps that are going to be tackled in this research are: (i) the development of a systematic framework for operability analysis using Gaussian Processes (GP), a type of supervised machine learning technique to handle general nonlinear and large-scale process models. This approach focuses on maintaining the representation of inherent nonlinearities of the underlying process aided by a GP surrogate instead of the computationally expensive, first-principles model. In addition, the use of GP regression opens the opportunity of using real plant data to develop a surrogate that can be used for operability analysis when a first-principles model is not readily available. Lastly, due to GP intrinsic roots in Bayesian inference, the uncertainty of the operability sets obtained can also be quantified. (ii) Development of an inverse mapping approach using the implicit function theorem and automatic differentiation. Recent innovations and advances in automatic differentiation allow the use of the implicit function theorem and a simple integration scheme to directly obtain the inverse map of a given process. This circumvents the use of NLP solvers, reducing the computational effort while maintaining accuracy. (iii) A framework that systematically uses operability analysis to deal with control structure selection in plantwide systems will be developed. This allows the systematic ranking of control structures based on their process operability characteristics.

Broader Impacts: Contributions related to the systematic operability analysis of large-scale, high-dimensional systems are made more tractable with the developed algorithms in this dissertation. The use of supervised machine learning, automatic differentiation and approaches for efficient evaluation of inherent combinatorics in large-scale process systems are pertinent contributions that are not well-addressed currently in process operability research. This directly impacts the application of process operability techniques in the industry since the algorithms and approaches developed in this dissertation potentially enables the use of the operability research in large-scale applications. Lastly, the development of an open-source process operability package in Python, namely *PyPO* (From Python-based Process Operability package) also provides ease-of-assess of all developed operability algorithms to users in a single-bundle fashion, and in a freely available programming language.

1 Overview and Objectives

In process systems engineering (PSE), process operability analysis has been developed as a systematic approach to quantifying simultaneous design and control objectives of a chemical/industrial process early in the conceptual phase. This approach can potentially enable the design of a process that when operated in practice, has a higher chance to be operable (i.e., capable of performing the overall objectives that were conceptualized initially). To analyze the operability of any given process model, operability analysis involves mapping tasks either in the forward or inverse directions, to obtain regions in the Cartesian system that will give insights into the feasibility and operability of the system studied. However, chemical process models of industrial scale are typically described mathematically as complex systems of nonlinear equations that might be also implicit. In addition, nonlinear constraints might be inherent to the mathematical description of these systems, as well as input and output multiplicities may be present in the solution. Therefore, systematic approaches for the efficient mapping using operability analysis are needed to address these challenges.

This research aims to develop efficient mapping techniques for process operability based on emerging tools and techniques from the literature, bridging the gap between classical operability theory and modern available tools. The underlying hypothesis is that efficient mapping techniques are the root cause of the main issues in operability analysis, and thus the development of robust mapping algorithms and approaches tailored for PSE applications will enhance the operability framework capabilities to deal with complex process models. To achieve this goal, the overall objective of this work is structured through the execution of the following specific aims:

Specific aim #1: Development of a machine learning-based process operability framework using Gaussian Processes (GP). By employing a Gaussian Process-based operability framework to systematically analyze the operability sets, the representation of the inherent nonlinearities of chemical processes is obtained while reducing the computational time when performing the forward and inverse mapping tasks. In addition, the intrinsic roots of GP in a Bayesian framework allow for accurate uncertainty quantification of the operability sets. Lastly, the use of supervised machine learning opens scientific venues to use data-based models whenever a first-principles model is not readily available.

Specific aim #2: Formulation of a framework for the inverse mapping evaluation employing the implicit function theorem and automatic differentiation. A framework for efficient inverse mapping to address the inverse problem inherent in process operability analysis is developed as an alternative to nonlinear programming-based (NLP-based) inverse mapping. The proposed framework takes advantage of recent differentiable programming advances through automatic differentiation formulation and algorithms. By employing the implicit function theorem and path integration, a direct way of dealing with the inverse mapping without recurring to an NLP is provided.

Specific aim #3: Establishment of an operability analysis framework for control structure selection. A framework that uses operability analysis principles and metrics will be developed to tackle the combinatorial explosion present in the control structure selection problem. The expectation is that the proposed approach will be able to rank control structures based on their operability characteristics.

Specific aim #4: Application of the proposed approaches to industrial chemical systems. The developed algorithms and frameworks will be applied to representative process models from the chemical industry. Such examples range from low to high dimensionality and considerable nonlinearity, to thoroughly test the capabilities of the proposed methods.

2 Expected Significance

The developed methods and algorithms will contribute to unifying the mapping of operability sets into a more generalized approach in terms of dimensionality and nonlinearity. In addition, the computational algorithms generated are expected to be efficient in terms of time and accuracy when compared to typical operability approaches for obtaining operability sets and inverse mapping. Moreover, the implementation of a framework for operability analysis seeking control structure selection opens a new venue for deciding control structures according to their overall achievability features, independent from the nature of the control laws implemented in the chemical process of focus. Overall, this research generates versatile algorithms that are not only generalizable but scalable and systematic as well, that will be compiled into a single Python library, namely *PyPO*.

3 Literature Review

Process operability has been developed in the last two decades as a valuable tool for qualitatively and quantitatively assessing the design and control interface of industrial processes, subject to expected disturbances and process constraints. Process operability has been extensively applied to steady-state systems and later extended to dynamic processes [1], [2].

Since the inception of process operability concepts [3], [4], several contributions have been made towards addressing the inherent challenges that emerged with the input-output operability mapping of the processes studied. Such challenges include nonlinearity, high-dimensionality and input-output multiplicity of process models that are derived to represent chemical/energy processes. Particularly in the field of process operability, response surface modeling (RSM) was proposed for reducing the complexity of operability calculations for high-dimensional systems [5]. Additionally, the operability concepts were extended for the analysis of plantwide systems by selecting production rate and product purity as the key variables of focus [6]. More recently, a series of nonlinear programming (NLP)-based approaches were developed to evaluate the feasibility of achieving desired outputs and calculate what should be the respective inputs to accomplish this goal [7]–[9]. In addition, these same studies [7]–[9] extended the operability framework to consider the concepts of process intensification and modularization, as a step forward towards using the operability tools for enabling modular manufacturing. Moreover, mixed-integer linear programming (MILP)-based methods were introduced [2], [10] employing computational geometry concepts for evaluating the operability regions for process design and intensification. Finally, the main process operability algorithms developed for intensification and modularization were compiled into an open-source Operability App in MATLAB [2] with a user-friendly interface for easy dissemination of the process operability algorithms.

Despite of these past contributions to the process operability field, the challenge regarding tackling nonlinear problems with high-dimensionality using first-principles models [9], [11] still remains. This task becomes computationally intractable as it grows in complexity with problem dimensionally, creating the need of recurring to parallel computing [11], an approach that is not always readily available and highly dependent on the computational infrastructure and modeling platform/numerical package used by practitioners or academic researchers. For such challenging high-dimensional applications, the idea of substituting the nonlinear first-principles process model by a surrogate model can be appealing to perform the operability computations in a more efficient manner. In particular, the NLP-based operability approaches [8], [9], [11] for process design and intensification could benefit of computational time reductions enabled by machine learning-based methods. Moreover, communication challenges have also been reported between process simulation platforms (e.g., Aspen Plus) and numerical packages that are required to perform process operability calculations (e.g., MATLAB or Python) [11].

The inverse mapping task for operability calculations consists of an inverse problem itself, which can be ill-posed according to Jacques Hadamard [12], [13]. Particularly, in process systems engineering (PSE), inverse mapping has been applied to investigate the process operability and achievability of modular designs of chemical processes, aiming higher efficiency and process footprint reduction as intensification targets [2], [7]–[11], [14]. Practical examples that are related to inverse mapping theory include: general parameter estimation problems (linear/nonlinear regression) [15] that permeates all fields of science, computed tomography reconstruction [16] and even the reconstruction of the image of a black-hole [17]. In process control, applications of control structures based on inverse models have also been developed [18], [19] using either the first-principles models or neural networks, as examples of inverse model dynamics applied to chemical processes. Moreover, optimization frameworks were recently developed using machine learning formulations [20] to solve general-purpose optimization problems in which inverse problems can take advantage of such formulations. Thus, inverse mapping presents itself as a vital concept in science in general with relevant applications to PSE. Therefore, there exists a particular need to investigate alternative ways of obtaining the inverse map of operability sets, revisiting the problem fundamentally.

The control structure selection problem deals with the selection of a subset of a large available set of candidate controlled variables (CVs) associated with the degrees of freedom as manipulated variables (MVs)[21]. This problem has been studied extensively in self-optimizing control research [22]–[29]. However, in process operability, there is no reported work in trying to deal with the inherent combinatorics of the control structure selection problem, limiting itself only to works related to proof of the independence of the operability index (OI) concerning the inventory control layer in plant-wide systems [3] and formalizing operability sets to reduce the dimensionality of plantwide processes [6]. Therefore, there is a gap in the state-of-the-art operability analysis and the optimal selection of controlled variables considering inherent operability features.

4 Background

4.1 Process Operability

Process operability has emerged as a viable alternative to the sequential tasks of assessing process design and control, by integrating both tasks in the early design phase of industrial processes [1], [2]. To perform this task, process operability tools were developed to quantify the achievability of process control objectives, given the available limits imposed on the input variables, while considering process constraints and expected disturbances that may occur during process operations [3]. In this section, process operability definitions for the case where the disturbances are kept at their nominal values are presented. For a complete and in-depth discussion on the previous operability concepts, including the presence of disturbances acting on the process, one must refer mainly to [2]–[4], [30].

To perform the operability analysis, the main requirement is that a process model that describes the relationship between the input (manipulated and/or disturbance) and output variables must be available [4]. A process model, M , with m inputs, p outputs, q disturbances and n states, can be defined as in Eq.1.

$$M = \begin{cases} \dot{x}_s = f(x_s, u, d) \\ y = g(x_s, u, d) \\ h_1(\dot{x}_s, x_s, y, \dot{u}, u, d) = 0 \\ h_2(\dot{x}_s, x_s, y, \dot{u}, u, d) \geq 0 \end{cases} \quad (1)$$

In which $u \in \mathbb{R}^m$ are the inputs, $y \in \mathbb{R}^p$ are the outputs, $d \in \mathbb{R}^q$ are the disturbances and $x_s \in \mathbb{R}^n$ are the state variables. Also, f and g are nonlinear maps and h_1 and h_2 correspond to equality and inequality process constraints, respectively. Based on the process model and associated variables, operating spaces/sets were established for the operability calculations and quantification of the operability index (OI) [4]. These sets are summarized with proper descriptions, acronyms, and mathematical formulations in Table 1. Refer to references [3], [4] for further details on these sets and other operability definitions. Figure 1 illustrates the main process operability spaces and the definitions. In Figure 1 (A), the lower and upper bounds for the manipulated/design variables are defined within the AIS. By evaluating these inputs through the process model (M), the outputs are calculated generating the AOS (B). From the desired operation with respect to such outputs, the DOS can be defined (C). The feasible portion of the DOS that is contained within the AOS is specified as the DOS* (C). Lastly, the DIS can be obtained via an inverse mapping (M^{-1}), in which its intersection with the AIS is defined as the DIS* (D).

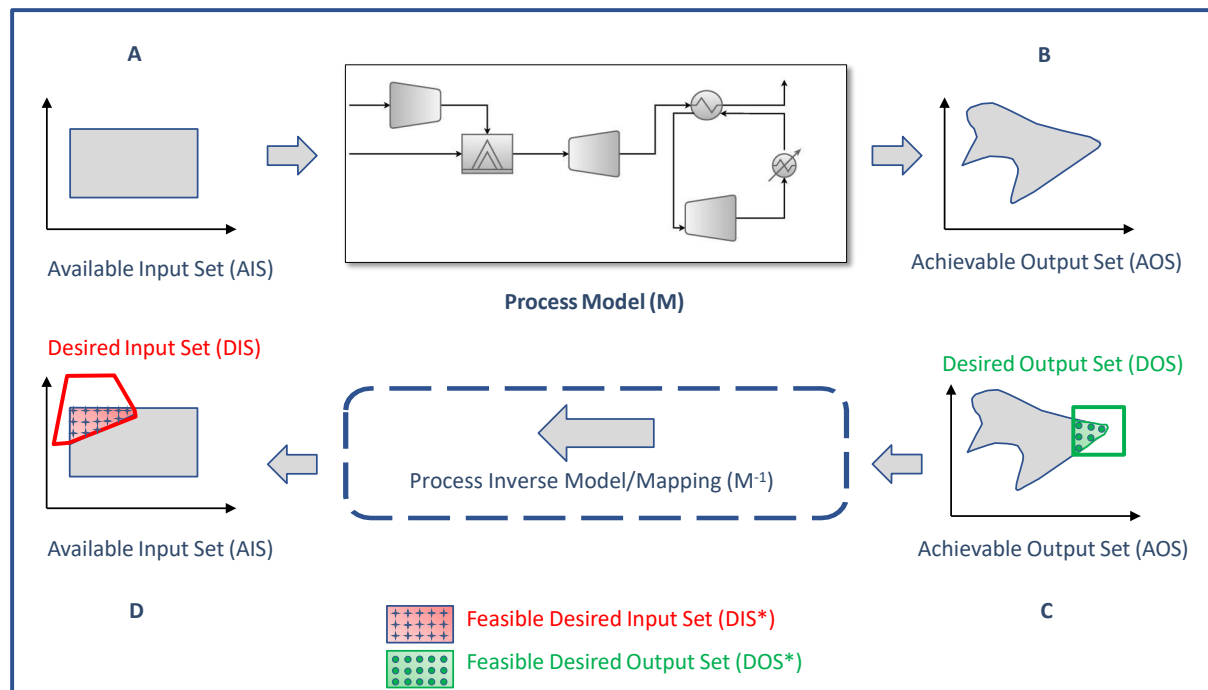


Figure 1: Visual exploration of main process operability sets and definitions.

Table 1: Steady-state operability sets: definitions and mathematical formulations.

Operability Set	Description	Mathematical Formulation
Available Input Set (AIS)	Manipulated inputs ($u \in \mathbb{R}^m$) based on the design of the process that is limited by the process constraints [3].	$AIS = \{u \mid u_i^{\min} \leq u_i \leq u_i^{\max}; 1 \leq i \leq m\}$
Expected Disturbance Set (EDS)	Disturbance variables ($d \in \mathbb{R}^q$) that can represent process uncertainties and variabilities.	$EDS = \{d \mid d_i^{\min} \leq d_i \leq d_i^{\max}; 1 \leq i \leq q\}$
Achievable Output Set (AOS)	Range of the outputs ($y \in \mathbb{R}^n$) that can be achieved using the inputs inside the AIS and disturbances within the EDS.	$AOS(d) = \{y \mid y = M(u, d); u \in AIS, d \text{ is fixed}\}$
Desired Output Set (DOS)	Production/target/efficiency requirements for the outputs that do not necessarily meet the ranges of the AOS.	$DOS = \{y \mid y_i^{\min} \leq y_i \leq y_i^{\max}; 1 \leq i \leq n\}$
Desired Input Set (DIS)	Set of inputs required to reach the entire DOS, given a disturbance vector d .	$DIS(d) = \{u \mid u = M^{-1}(y, d); y \in DOS, d \text{ is fixed}\}$
Feasible Desired Output Set (DOS*)	Feasible set of desired outputs calculated via relative error minimization from the DOS using for example the NLP-based approach [9].	$DOS^* = \{y^* \mid y^* = M(u^*); u^* \in DIS^*\}$
Feasible Desired Input Set (DIS*)	Optimal set of inputs that are required to obtain the Feasible Desired Output Set (DOS*), calculated for example via the NLP-based approach.	$DIS^* = \{u^* \mid u^* = (u_1^*, u_2^*, u_3^* \dots u_i^*)\}$ $i \stackrel{\text{def}}{=} \text{Discretized DOS grid size}$

Especially for process design and intensification purposes, it is important to note that the task of obtaining the inverse model/mapping (M^{-1}) is of paramount importance. As stated above, high-dimensionality, non-linearities, input-output multiplicities, and additional challenges such as infeasibility of the desired targets [2] are the most common issues to be faced when performing this task. In order to circumvent these issues, linear and nonlinear programming-based operability methods were successfully developed [9], [10], respectively. Focusing on the latter, namely the NLP-based approach, further definitions regarding the feasibility of the desired input and output sets were created. Instead of analytically calculating (M^{-1}), the work in [9] proposed an NLP-based optimization problem to calculate the discretized inputs from a specified DOS, using an objective function defined by a relative error minimization. More specifically, the approach consists of finding a Feasible Desired Input Set (DIS*) that results in a Feasible Desired Output Set (DOS*), with the latter being optimized to be as close as possible from the original DOS. For the optimization problem of the NLP-based approach, the error minimization function can be formulated considering the process required constraints, intensification/efficiency targets and solved sequentially or by using a bilevel programming approach, as showed in [9]. The possible optimization problems of this approach are adapted in this work for the use of GP responses as a surrogate, and are discussed in depth in the Preliminary Results section below.

With the input-output sets defined above, the operability index (OI) can be calculated as shown in Eq.2. A process is considered fully operable when the OI is 1 and if it is less than 1, some regions of the DOS are not achievable [1].

$$OI = \frac{\mu(AOS \cap DOS)}{\mu(DOS)} \quad (2)$$

In which μ indicates the measure of regions, varying depending on the dimensionality of the considered sets, for example length for 1D systems, area for 2D systems, volume for 3D systems and hypervolumes for systems of higher dimensionality [2].

4.2 Gaussian Process (GP) Regression

GP models are employed in this work as a surrogate to the process first-principles or simulation-based models. The Gaussian Process implementation used thus far in this dissertation is based on the work of [31], [32] and similar approaches can be found in [33], [34]. For historical purposes, the works by [35] and [36] are also recommended. For a thorough discussion on the subject, refer to [36]–[38].

Considering a set of g experiments, $S = [u_1 \dots u_g]^T$, with $u_i \in \mathbb{R}^m$ (input variables), and an output vector, $Y = [y_1 \dots y_g]^T$, a GP is capable of representing a nonlinear function $Y(u) \in \mathbb{R}^p$, with the aid of two terms: a regression (\mathcal{F}) (also known in the literature as mean [32], [39], $\mu(u)$) and a stochastic function (z) (also known as kernel function [32], [39], $K(u)$) as shown in Eq.3.

$$\hat{Y}_l(u) = \mathcal{F}(u) + z_l(u), \quad l = 1, \dots, p \quad (3)$$

The regression model is considered as a linear combination of functions $f_j : \mathbb{R}^m \rightarrow \mathbb{R}$, and typically the regression functions used are polynomials of orders zero to two [32], [36]. Additionally, it is assumed that each z_l has zero mean with covariance between any two given points, u and u' as in Eq.4.

$$\text{Cov}[z_l(u), z_l(u')] = \sigma_l^2 \mathcal{R}(\theta, u, u'), \quad l = 1, \dots, p \quad (4)$$

In which σ^2 is the process variance for the l^{th} output and $\mathcal{R}(\theta, u, u')$ is a correlation function. There are several correlation functions developed for GP models in the literature [31], [32], [39]. For the sake of simplicity and given the particular characteristic of being continuously differentiable, in this work, the correlation function assumed is of the form known as squared-exponential or Gaussian form ($p_j = 2$) as shown in Eq.5.

$$\begin{aligned} \mathcal{R}(\theta, u, u') &= \prod_{j=1}^m \mathcal{R}_j(\theta, u_j - u'_j), (\theta \geq 0) \\ \mathcal{R}_j(\theta, u_j - u'_j) &= e^{(-\theta_j(u_j - u'_j)^{p_j})}, (p_j = 2) \end{aligned} \quad (5)$$

In which θ are defined as hyperparameters and their values can indicate if the inputs are highly correlated or not [40] and also how fast the correlation goes to zero as the process moves in the j^{th} coordinate direction [33]. The parameter p_j represents the smoothness of the correlation [36], and reducing its value increases the rate at which the correlation initially drops as the distance between two given points $(u_j - u'_j)$ increases [36]. When $p_j \approx 0$, there is a discontinuity between $\hat{Y}(u_j)$ and $\hat{Y}(u'_j)$ [41], excluding the possibility of correlation between two given arbitrary points. Finally, the determination of the hyperparameters θ is a result of an optimization problem with the optimal solution corresponding to the maximum likelihood estimation [32], where $|R|$ is the determinant of the correlation matrix R , as in Eq.6.

$$\min_{\theta} \left\{ \psi(\theta) \equiv |R|^{\frac{1}{\theta}} \sigma^2 \right\} \quad (6)$$

4.3 Control Structure Selection

Control structure selection is a vast field of study that encompasses the task of selecting controlled variables (CVs) and manipulated variables (MVs), as well as the pairings between such variables [21]. When dealing with a chemical plant, a considerable amount of measurements are available, each being a potential CV to be used in a control loop using a respective MV. This task has combinatorial properties as discussed in the literature [22], [24]. Studies in the 1980s and 1990s have been reviewed in [42] based on controllability and achievable performance that lead to CVs that are easy to control but do not necessarily guarantee the overall objectives of the plant [21]. In plantwide control and self-optimizing control [22], [40] this problem is well-studied, using the economic loss generated by a feedback control policy as a metric for selecting the CVs. This yields to the analysis with using the economic loss exclusively as a metric for ranking candidate-controlled variables among a large subset. Several examples and applications have been tested using this approach such as hydrodealkylation (HDA) [23], and ammonia synthesis [24] to name a few. A detailed review of applications that take advantage of self-optimizing control concepts to deal with the control structure selection problem is available in [43]. As an illustrative example, reference [23] shows that for the HDA process, with 13 degrees of freedom (MVs) and 70 measurements (CV candidates), there are $\binom{70}{13} = 70!/13!57! = 4.7466 \times 10^{13}$ control structures, excluding alternative inventory control strategies that are also available. Clearly, this can be considered as an NP-hard problem due to its combinatorial properties, drawing the attention of researchers in trying to tailor algorithms to quickly assess the overall subset of CVs and rank them accordingly using minimum singular value criterion, Hankel singular values or the self-optimizing control loss as a measure [25]–[29], [44], [45].

Irrespective of the works in the field of plantwide control, in process operability, the only works that try to link these research fields are when proving the independence of the operability index (OI) from the inventory (regulatory) control layer [46] and the definition of operability sets for key variables in plantwide processes [6], with none of which mentioning the combinatorics inherent to control structure selection in large-scale systems. This leaves a gap since the control structure selection problem might

benefit from a more comprehensive metric that assesses process controllability and flexibility in terms of the plant's overall objectives when ranking competing control structures, such as the operability index (OI).

5 Preliminary Results

Results associated with all aims were produced thus far. Regarding Aim #1, a full approach for using GP models coupled with process operability analysis was developed and tested using case studies of increasing dimensionality, ranging from a 2x2 (inputs x outputs) membrane reactor to an 8x3 natural gas combined cycle plant (NGCC) application. These results are detailed in one of the peer-reviewed publications that are a product of this dissertation [47].

For Aim #2, a full approach for inverse mapping using automatic differentiation has been proposed and shown to be effective with respect to computational time and accuracy when compared against traditional inverse mapping techniques employed in operability analysis. A continuous stirred tank reactor (CSTR) and a membrane reactor for direct methane aromatization were used as case studies. Details of this work are available in [48].

For Aim #3, an operability analysis framework for plantwide control structure selection has been developed and the preliminary results show that process operability analysis and more specifically, the operability index (OI), can be used as a tool to rank control structures. A depropanizer distillation column, a common unit operation in refineries, is used as a case study.

Lastly, for Aim #4, the following case studies representative of industrial processes were used throughout the approaches developed: Continuous stirred tank reactor (CSTR), direct methane aromatization membrane reactor for natural gas conversion (DMA-MR), natural gas combined cycle power plant (NGCC) and a depropanizer distillation column. All case studies are process models that have inherent strong nonlinearity due to conservation laws, kinetics and thermodynamic equations of state. In addition, such case studies range from different dimensionalities up to problems of combinatorial nature.

Specific preliminary results for all these aims are summarized below.

5.1 Aim # 1: Machine Learning-based Process Operability Framework Using Gaussian Processes (GP)

The proposed method is depicted in Figure 2 and is discussed step-by-step in the publication [47] that was generated as a result of this aim. The main objective is to develop a systematic and generalized method capable of performing prior process operability calculations [9], [10] while maintaining accuracy and reducing computational cost. In addition, the proposed method should be able to tackle systems of any dimensionality that present strongly nonlinear behavior, challenges that can be addressed with the help of the GP models. Moreover, this method should facilitate the employment of the process operability algorithms, avoiding the need of coupling process modeling tools with numerical packages, as the surrogate model can be used instead of a first-principles/process simulator model.

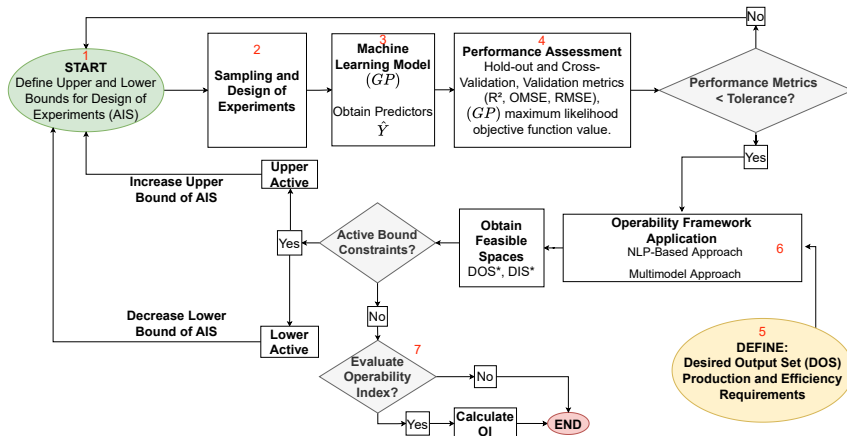


Figure 2: Flowchart with the proposed method steps for GP model-based operability analysis [47].

5.1.1 Direct Methane Aromatization Membrane Reactor (DMA-MR)

This first example consists of the steady-state analysis of the Direct Methane Aromatization Membrane Reactor (DMA-MR) for hydrogen and benzene production. This process has been studied as an application of process intensification and modularization of natural/shale gas processing [7], [8]. A schematic of the DMA-MR process is depicted in Figure 3, in which reaction and separation are combined in a single equipment, increasing the overall system efficiency and potentially reducing the footprint of this chemical process [10]. The DMA-MR model consists of a system of 8 ordinary differential equations (ODE), corresponding to the molar balances for the species involved in the two-step reaction mechanism that takes place in the tube side. Some of the species permeate to the shell through the membrane, mainly H_2 , shifting the equilibrium towards the formation of products (by Le Chatelier's principle). The full mathematical description of the DMA-MR model is readily available in the literature [9], including the first-principles model assumptions that lead to such molar balances [9].

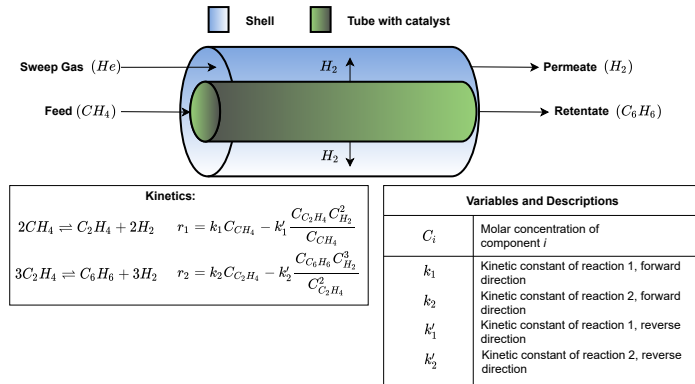


Figure 3: DMA-MR schematic.

The first application example consists of a 2×2 (inputs x outputs) subsystem associated with this DMA-MR process. Despite of the low system dimensionality in this example, this process model is highly nonlinear due to the presence of the nonlinear reaction kinetics and the membrane flux in the intensified unit. Such nonlinearities make the inverse operability mapping task challenging, and thus this system serves as a good candidate for benchmarking the computational time and accuracy of the proposed methods, when compared to the results of the nonlinear operability methods that are readily available in [7], [8].

For this application, a GP model is created using as input variables the tube diameter and tube length, corresponding to the variables in the AIS. Also, for the DOS, the variables considered are the methane conversion (X_{CH_4}), and the production rate of benzene ($F_{C_6H_6}$). After generating the GP models and validating them, such models are employed to obtain the inverse mapping for operability and subsequently, the DIS*-DOS* calculations. For comparison purposes, both the NLP-based approach for inverse mapping and the multimodel approach for OI calculation are employed using the nonlinear first-principles and the GP-based models, as shown in Figures 4 and 5, in which both tasks were performed with accuracy. Note from these figures the small error obtained when comparing the original nonlinear first-principles model against the GP-based model responses for operability. Table 2 shows the relative errors between these model responses for the membrane reactor modular design, confirming the agreement between the responses obtained.

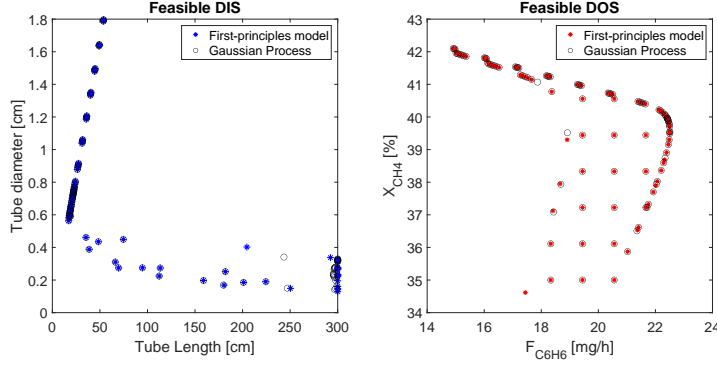


Figure 4: DIS* and DOS* comparisons: calculations employing GP model versus original first-principles nonlinear model.

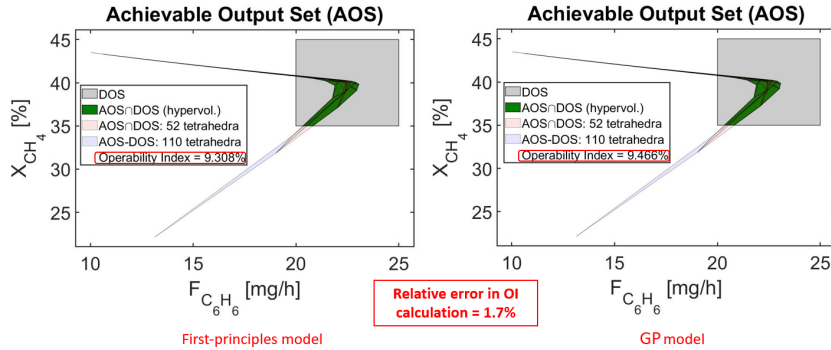


Figure 5: OI calculations using first-principles model versus GP-based model. Small relative error of 1.7% is obtained between calculations.

Table 2: Relative errors between nonlinear-based and GP-based NLP operability approaches for calculating intensified design variables.

Intensified design variable	Nonlinear model	GP	Relative error [%]
Tube length [cm]	17.2283	17.2205	0.0454
Tube diameter [cm]	0.5634	0.5636	0.0388

The overall computational time for obtaining the results in Table 2 when using the first-principles nonlinear model for this 2x2 system was of 5 min 38s. It has been shown previously that the computational time for this system is expected to grow exponentially with problem dimensionality [11]. However, the overall computational time associated with the GP-based method (generation of 2000 points for the input-output mapping, fitting the GP responses and running the optimization problem) was of 58 seconds. This represents a decrease of 5.8 times in computational time. If this computational time evaluation was done considering only the process operability calculations when using the GP-based approach against its nonlinear model-based counterpart, this difference becomes even larger. The required time to obtain the operability sets using the GP-based approach is of only 0.0477s against the 5 min 38s previously mentioned for the nonlinear model-based method, thus reducing the computational time by about four orders of magnitude. For comparison purposes, a previous algorithm developed employing Mixed-Integer Linear Programming (MILP) for process operability calculations [14] achieved reduction of computational time of 3.051 times and relative error of 1.28% with respect to the membrane area calculated using the tube length and diameter as input variables, considering the same case study as in this work. Hence, the proposed approach in this work has the potential to enable operability calculations for high-dimensional systems that would not be possible otherwise. Also, the results above show that the accuracy of the proposed method for generating the input-output mappings for operability analysis was not compromised, while the complexity of calculating such inverse mappings was reduced.

5.2 Aim #2: Framework for the Inverse Mapping Evaluation Using The Implicit Function Theorem and Automatic Differentiation

The proposed approach for inverse mapping evaluation is depicted in Figure 6 and is discussed thoroughly in the publication that was generated as a result of this aim [48]. The steps taken in this approach are outlined in Figure 6.

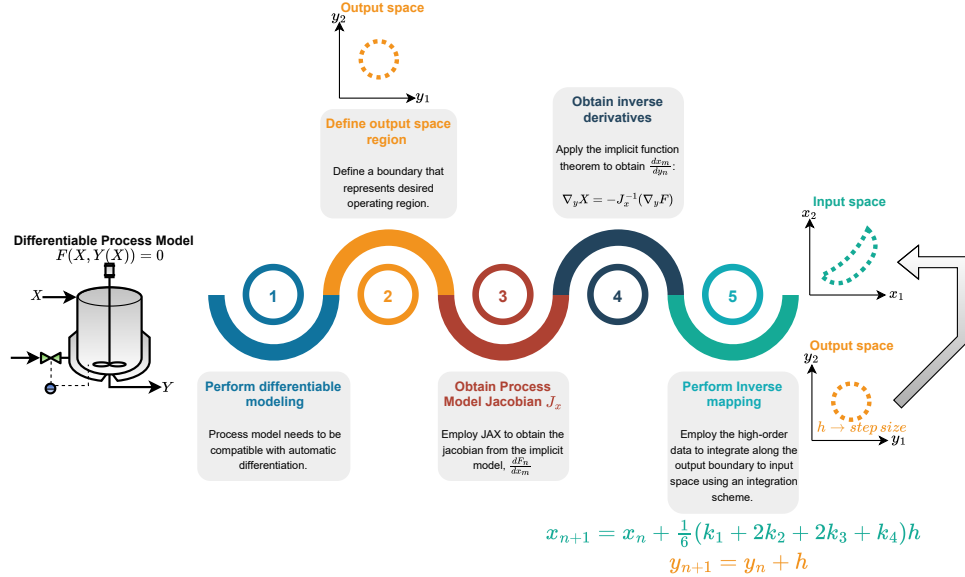


Figure 6: Flowchart of proposed method for AD-based inverse mapping [48].

After employing the steps outlined in Figure 6, the input space region is obtained, giving insights about operating regions associated with a desired specification given in the output space. The main advantage of the proposed approach is that it performs direct calculations from the output to input spaces, circumventing the use of optimization algorithms for instance. In addition, the use of AD might enhance the accuracy of a given solution (assuming that there is a sufficiently efficient integration scheme) and can be calculated rapidly using JAX [49], when comparing to finite-differences schemes for obtaining high-order data (Jacobians and Hessians).

Despite the robust features of the proposed method, potential issues might be the possibility of model discontinuities, in which the AD package would indicate elements of J_x being defined as “NaN” (*Not a Number*) or as “ $\pm inf$ ” (*infinity*). In that case, it is suggested that further investigation of the output space region be performed since this issue might be possibly related to infeasibility of the proposed output space region (e.g., there is no solution for this given output space) or the inverse problem might be simply ill-posed in Hadamard’s sense [15]. Lastly but not less important, bifurcations may be inherently present in the solution of the inverse mapping, being shown as the Jacobian at the evaluated point as singular. In this particular case, continuation methods such as arc length-based [50]–[52] for instance are essential to circumvent this potential challenge. When using arc length continuation, the problem is reparametrized in terms of an arc-length [53], allowing the computation of the Jacobian in this augmented system to be nonsingular. This way, the inverse map can be done throughout the solution branch in its entirety without failing.

5.2.1 DMA-MR Example

The DMA-MR case study is revisited here to show the capabilities of the proposed approach for inverse mapping. The main objective of this case study is to apply the proposed approach to the required inverse mapping using the process operability sets for analysis and compare against the NLP-based approach [7], [8].

The main issue to be addressed in the design and manufacturing of this process is to have a modular design able to meet the minimum specifications of benzene production (a value-added chemical) and acceptable methane conversion, which might allow for on-site conversion of natural gas. More fundamentally, an inverse mapping naturally arises and it is required as the benzene production and methane

conversion belong to the output space, and conversely, the design specifications of the DMA-MR are inputs to the forward mapping. This problem must be numerically integrated since there is no analytical solution to the forward problem. As long as the numerical integration scheme is differentiable, one can use the proposed approach to solve the inverse problem.

For this case study, the DMA-MR model equations have to be rewritten to be JAX-compatible, developing a differentiable model (following Step 1 in Figure 6) in which high-order data (e.g, the derivatives) can be obtained to be used in the proposed approach. To integrate the system of ODEs, a differentiable version of the Dormand-Prince method available in JAX was used [49].

The output space is defined as a circle-shaped DOS region, which encapsulates the desired range of benzene production and methane conversion of 22.3 – 23 [mg/h] and 39.2 – 40 [%], respectively. After defining the DOS, its boundary region is discretized using an equally spaced vector of 100 points. Consecutively, the proposed approach is applied and the inverse mapping is obtained for the DIS region that corresponds to the boundary of possible designs that will attain to the specifications of the DOS. The results obtained can be inspected in Figure 7.

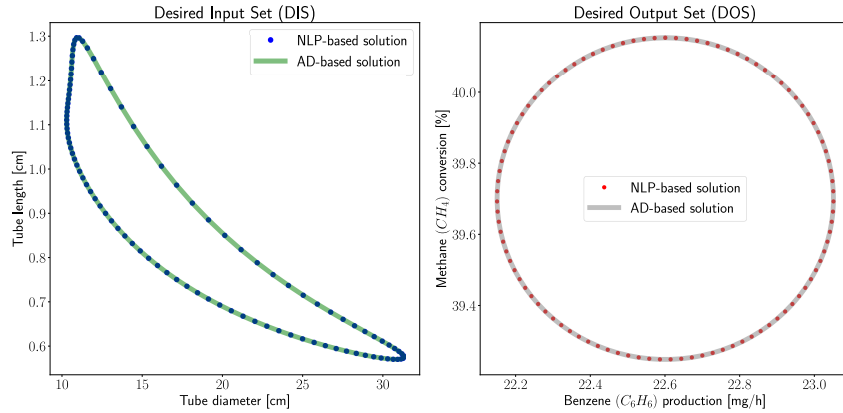


Figure 7: Comparison of inverse mappings obtained: NLP-based approach vs proposed approach.

An initial inspection of Figure 7 indicates that despite of having a well-defined output space (DOS) region, the inverse problem maps to a non-convex and nonlinear desired input space (DIS). This result is expected as inverse problems are typically ill-posed (following Hadamard’s definition of what a well-posed problem might be) with respect to stability conditions [15] of a given solution.

Moreover, the inverse map solution obtained via the proposed approach is compared to the NLP-based approach [7]–[9] developed for process operability calculations with respect to accuracy and computational time. The results of such comparison can be visually inspected in Figure 7, showing the agreement between both approaches, which indicates that the proposed approach is capable of effectively performing the inverse mapping task. The NLP-based approach for model inversion was also run using a “warm-start” strategy (that is, the solution of the previous run is used as an estimate to the subsequent run). Lastly, a third implementation was done in which the derivatives needed for solving the NLP are obtained using JAX.

The computational time required for the proposed approach against these methods is significantly reduced as it can be examined in Table 3. For instance, the proposed approach is about 19.2 times faster when compared to a naive implementation of the NLP-based approach solved using IPOPT with finite differences (default option) and “cold-start” which can be computationally expensive depending on the nature of the NLP problem.

Table 3: Computational time for DMA-MR inverse mapping: NLP-based approach *vs* proposed approach.

Solution approach	Time [min]	Decrease w.r.t NLP implementation [times]
NLP-based (“cold-start” + finite differences)	17.84	19.18
NLP-based (“warm-start” + finite differences)	11.56	12.43
NLP-based (“warm-start” + AD)	1.97	2.11
Proposed approach in this work	0.93	-

Now comparing to a state-of-the-art implementation of the NLP-based approach which uses AD for obtaining the derivatives and a “warm-start” strategy, the computational time decrease between the NLP-based approach and the one proposed in this work becomes narrower. However, the proposed approach is still able to be 111% faster. This can be explained by the fact that the proposed method in this work relies exclusively on first-order data (that is, the Jacobian) while the NLP-based method needs first and second-order data (Jacobian and Hessian). Moreover, the numerical integration is a simpler, more direct approach to obtain the solution rather than using a full NLP-based solution, even if one is using AD and a “warm-start” strategy.

Lastly, the analysis of derivatives and vector fields were also addressed in the research publication generated by this aim and can be found in details in [48], as well as tables indicating the numerical values for error comparisons being low.

5.3 Aim #3: Operability Analysis Framework for Control Structure Selection

The fundamental idea of using operability analysis for control structure selection is to employ the operability index (OI) as a measure of achievability of control structures, being able to rank them in terms of process operability. This way, the controlled variables (CVs) can be chosen at the conceptual design phase using a steady-state model of the process, guaranteeing that the CVs held constant maximize the operability of a given system. The main assumptions of the currently framework are:

1. There is integral action on the yet-to-be-implemented control structure: This assumption is needed since integral action guarantees no offset for reaching the steady states.
2. The process is governed by steady-state operation: Since a steady-state process model is used, it is implicitly assumed that its operation is governed by fixed set points instead of a trajectory (i.e., as opposed to batch operations, for instance).

The main steps of the proposed method are depicted in Figures 8-9 and discussed step-by-step in this section.

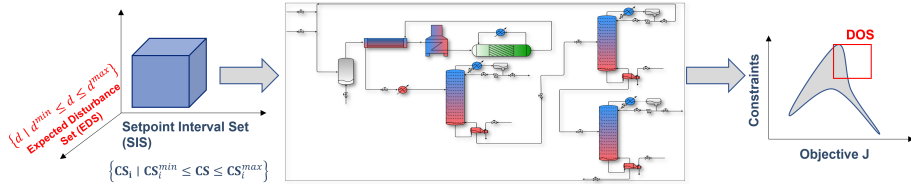


Figure 8: Steps 1-3: Defining one SIS for each control structure, the respective EDS for the overall process, and the plant overall objectives into the AOS/DOS.

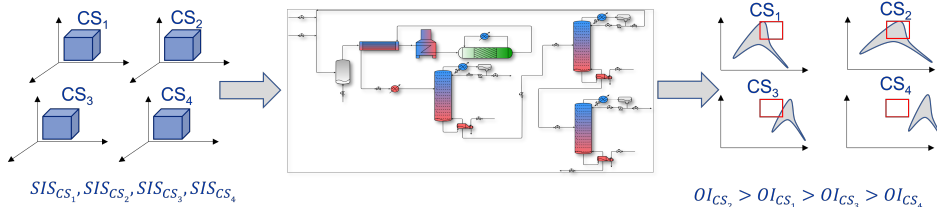


Figure 9: Steps 4-5: The process model is run for each SIS at all discretized setpoint values, and for each disturbance scenario in the EDS. With each AOS obtained for each SIS, the OI can be evaluated for each control structure and ranked in descending order.

The main steps of the proposed method are:

1. **Use the newly introduced Setpoint Interval Set (SIS) to quantify the achievability of the set control structures:** In this step, the i^{th} control structures CS_i are listed, and the ranges for each candidate controlled variable are defined. This way, each control structure will have one SIS.

2. **Define the AOS/DOS according to the plant overall objectives:** The objective in this step is to incorporate the main goals of the plant that is represented by the process model. Hence, the overall plant objective function and constraints related to product specification, pollutant emission and/or sustainability metrics are to be used in the dimensions of the AOS/DOS. The limits of the DOS are inherently a consequence of process knowledge, market demands and products specification. For example, one dimension of the DOS might be the plant's economic objective function that needs to maintain profitable operation. Another dimension might be the main product minimum purity, such as in distillation columns, or even the minimum conversion in a chemical reactor.
3. **Define EDS:** In this step, the EDS variables and their respective ranges are to be selected. This will guarantee that the proposed approach will evaluate the operability index (OI) for each control structure taking into consideration the effect of disturbances. This way, the control structures with the highest OIs inherently have better disturbance rejection capabilities. On the other hand, control structures with low values for the OI would be unable to reject the selected disturbances and need to be discarded.
4. **Run process model for each SIS and each disturbance in the EDS:** For each SIS and each EDS, the process model is run. The AOS is obtained, encompassing the overall plant's objective and compared against the DOS via the OI.
5. **Ranking of Control structures:** With all simulations complete, each control structure within each SIS will have a respective value for the OI. All SISs are then ranked in descending order and the control structure with the highest OI is selected to be associated with the degrees of freedom in the actual process.

In Figure 9, it can be seen in this illustrative example that control structure #2 (SIS_{CS_2}) has an AOS that intersects the highest with the DOS, followed by the first one SIS_{CS_1} , subsequently SIS_{CS_3} and lastly SIS_{CS_4} , which has no intersection with the AOS (OI of 0%), ranked as $OI_{CS_2} \geq OI_{CS_1} \geq OI_{CS_3} \geq OI_{CS_4}$. This process is general and it works in any dimension, although it is of combinatorial nature that still needs to be assessed automatically rather than by “brute-force”, which is running each case.

Lastly, a depropanizer distillation column is used as a case study to show the capabilities and plenimiray results obtained thus far.

5.3.1 Depropanizer Distillation Column

As an illustrative example, a depropanizer distillation column is used to test the proposed framework. This process has been studied in the context of Self-Optimizing Control (SOC) [22], [40], [41], for which the results can be analyzed and compared against. Instead of ranking control structures based on the loss incurred by not employing real-time optimization as is in SOC [22], here the control structures are to be ranked based on their operability characteristics quantified by the OI. The process is depicted in Figure 10, with all five degrees of freedom highlighted in red, and the system modeled in Aspen Plus.

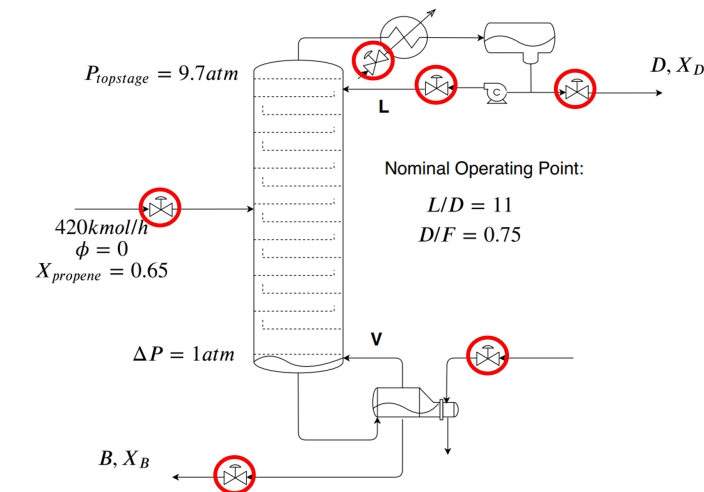


Figure 10: Depropanizer distillation column based on [22], [40], [41].

From the five available degrees of freedom, two need to be used to guarantee stable operation and have no steady-state effect, and the feed is considered as specified. Thus, there are two remaining degrees of freedom available to keep the process at the desired operation. Following [40], the economic operation per hour is given by Eq. 7.

$$J = 20D + (10 - 20x_B)B - 70Q_R [\$/h] \quad (7)$$

In which D and B are molar flow rates [$kmol/h$], x_B molar composition and Q_R the reboiler duty [GJ/h]. In addition, there is a purity constraint for propene, $x_D \geq 99\%$. The plant's objective function and the purity constraint will form the AOS/DOS. Their bounds are based on the nominally optimal operating point.

The next step is to select candidate controlled variables (CV) that will form each SIS. The following variables are selected and shown in Table 4 with no loss of generality, based on the literature [22], [40], [41].

Table 4: Candidate controlled variables (CV) for depropanizer case study.

Controlled Variable (CV)	Lower Bound	Upper Bound
Reflux ratio (RR) [mol basis]	10	15
Distillate-to-feed ratio (D/F) [mol basis]	0.6	0.9
Sensitive tray temperature (T_{133}) [$^{\circ}C$]	25	29
Reflux-to-feed ratio (L/F) [mol basis]	8.5	12
Boilup-to-feed ratio (V/F) [mol basis]	8.5	12

With five measurements and two degrees of freedom, there are

$$C_2(5) = \binom{5}{2} = \frac{5!}{2!(5-2)!} = 10 \quad (8)$$

possible control structures, which are the following:

$$\begin{aligned} CS_1 &= \left(\begin{array}{c} RR \\ D/F \end{array} \right), CS_2 = \left(\begin{array}{c} L/F \\ T_{133} \end{array} \right), CS_3 = \left(\begin{array}{c} RR \\ T_{133} \end{array} \right), CS_4 = \left(\begin{array}{c} V/F \\ T_{133} \end{array} \right), CS_5 = \left(\begin{array}{c} RR \\ L/F \end{array} \right), \\ CS_6 &= \left(\begin{array}{c} RR \\ V/F \end{array} \right), CS_7 = \left(\begin{array}{c} D/F \\ T_{133} \end{array} \right), CS_8 = \left(\begin{array}{c} D/F \\ L/F \end{array} \right), CS_9 = \left(\begin{array}{c} D/F \\ V/F \end{array} \right), CS_{10} = \left(\begin{array}{c} L/F \\ V/F \end{array} \right) \end{aligned} \quad (9)$$

For the DOS, the lower bound for the economic objective function is chosen to be the optimally nominal value reported in [40] of 2760\$/h with an upper bound of +25% of this value. The EDS is comprised of the propene flow rate in the feed under a $\pm 10\%$ variation. With the definition of all SIS sets representing each control structure, the EDS and the plant's desired operation represented in the DOS, each scenario is run to obtain the plant's AOS for each SIS. Then, the multimodel approach [10], [14] is used to evaluate the OI for each case, aided by the Process Operability App [2]. The results are depicted in Figure 11, which shows only the operable control structures.

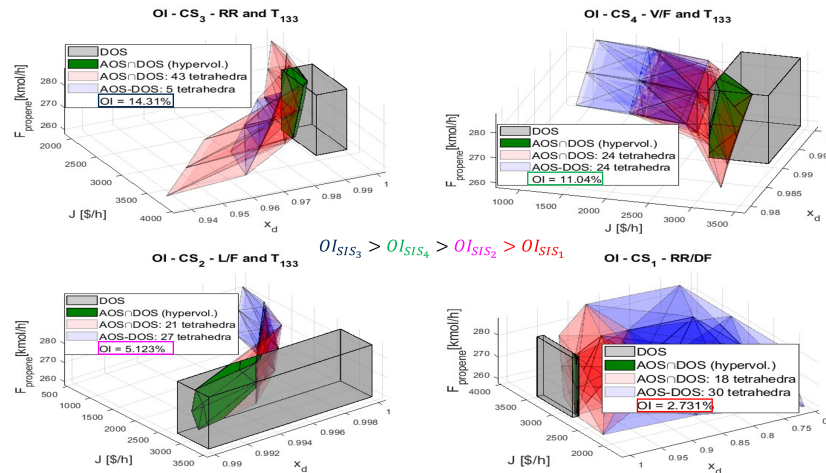


Figure 11: Operable control structures: $SIS_3 \geq SIS_4 \geq SIS_2 \geq SIS_1$.

For the first group (operable control structures), it can be seen that control structures using a sensitive tray temperature have higher operability index values, namely

$$SIS_3 = \begin{pmatrix} RR \\ T_{133} \end{pmatrix}, SIS_4 = \begin{pmatrix} V/F \\ T_{133} \end{pmatrix}, SIS_2 = \begin{pmatrix} L/F \\ T_{133} \end{pmatrix}, SIS_1 = \begin{pmatrix} RR \\ D/F \end{pmatrix} \quad (10)$$

This is an important result that validates the proposed approach since it is known that for distillation processes, the use of sensitive tray temperature has good control performance, as shown in [40], [54], [55]. These preliminary results show that process operability can be used to systematically assess promising control structures early in the design phase of a chemical process. More importantly, the proposed approach can be also used to safely discard control structures that do not ensure achievability of the plant's objectives, aiding researchers and practitioners to focus on the promising control designs, especially when dealing with plantwide problems in which the number of possible control structures suffering from combinatorial explosion.

6 Research Plan

A more detailed discussion of the goals and plans of this dissertation is shown in this section, as well as the necessary subitems to complete each aim.

Specific aim #1: Development of a machine learning-based process operability framework using Gaussian Processes (GP). Initially, as a proof-of-concept, low-dimensional systems were addressed, such as the DMA-MR shown previously. Then, the proposed framework was extended to high-dimensional studies, such as the NGCC plant that was modeled in a process simulation platform. Lastly, the use of GP uncertainty quantification will be explored as a representation of the expected disturbance set (EDS) for operability analysis

1. Development of the overall flowchart for GP-based operability framework (completed): The development of the main algorithm/approach for using GP models for operability calculations is developed in this step as described in Section 5.1.
2. Extension of the proposed framework for uncertainty quantification: GP models are capable of evaluating the uncertainty of the mean prediction of the surrogate model generated. Given this, the possibility of exploring this particular feature as a representation of the expected disturbance set (EDS) will be evaluated. The expectation is that the use of the uncertainty from a GP model will give confidence bounds for the operability study.
3. Extension of the proposed framework for dynamic operability: It is possible to perform a dynamic operability analysis [56] using a GP model in a nonlinear autoregressive model with exogenous inputs (NARX) scheme, known in the literature as GP-NARX [57]. The expectation is that this aim would allow for dynamic operability analysis to be performed in real-time, when dynamic data is available but a dynamic process model is not.

Specific aim #2: Formulation of a framework for the inverse mapping evaluation employing the implicit function theorem and automatic differentiation. Initially, the framework was proposed and tested for \mathbb{R}^2 systems, as a proof-of-concept. Then, the proposed approach will be generalized in terms of dimensionality and considering the multiplicity of steady states (input/output multiplicity) by incorporating bifurcation analysis into the proposed framework.

1. Conceptualize the proposed method and test it (completed): In this subtask, the proposed approach was conceptualized and formally defined in mathematical terms, which lead to what is shown in Section 5.2.
2. Extend it for high-dimensional, multiplicity-featured cases: The proposed method is to be generalized in terms of dimensionality, allowing its use in any \mathbb{R}^n dimension. In addition, it will be extended to cover the cases in which multiple solution branches are present in the inverse mapping task, by employing numeric bifurcation techniques, such as arc-length-based [53] ones.

Specific aim #3: Establishment of an operability analysis framework for control structure selection. This aim focuses on developing a framework that takes advantage of process operability concepts to evaluate competing control structures in a chemical process. The fundamental idea is to use this algorithm to rank the competing control structures according to their operability index and select those that are more operable based on the OI.

1. Conceptualize the proposed method and test it (completed): Initially, the proposed method was formulated and a new operability set named the Setpoint Interval Set (SIS) was defined to be able to analyze different setpoint ranges for the operability study of the control structures. The proposed approach was tested using a depropanizer distillation column and the results were compared against the literature for different control structure selection techniques.
2. Development of an automated search algorithm: The proposed method is to be automated as a linear program in the form of a branch-and-bound algorithm that uses as a monotonic criterion of pruning and branching the operability index itself. Therefore, it will automatically search and rank the control structures according to their operability indexes.

Specific aim #4: Application of the proposed approaches to industrial chemical systems. All mapping techniques are applied to representative, industrial-scale, chemical processes. All of the following systems have been considered:

1. DMA-MR (completed): The Direct Methane Aromatization Membrane Reactor (DMA-MR) is used among the two first aims since it has been used as a benchmark for operability mapping throughout the years [2], [7], [8], [10], [14], [47], [48], allowing the comparison against the proposed mapping techniques in this work.
2. NGCC (completed): The natural gas combined cycle is used as a high-dimensional case study that can be also directly used as a comparison against classical operability mapping techniques, validating the proposed approaches in this dissertation.
3. CSTR (completed): A motivating continuous reactor is used in Aim #2 to illustrate the concepts involving AD-based inverse mapping.
4. Depropanizer distillation column (completed): A depropanizer distillation column is used as a benchmark for the third aim since it has been studied particularly in plantwide control studies [22], [40], [41] and it corresponds to a representative, nonlinear typical unit operation present in oil refineries.
5. Additional plantwide, large scale, and high-dimension systems: As a last case study, a typical plant-wide process is to be used as a benchmark of the proposed methods. Candidates are the ethylbenzene process [58], an ammonia synthesis plant [24], and a steam methane reforming plant [59].

7 Timeline

Activities	2020		2021		2022		2023		2024			
	Aug-Dec	Jan-Jun	Jul-Dec	Jan-Jun	Jul-Dec	Jan-Jun	Jul-Dec	Dec-May	May-July			
Aim #1	Proposed approach		GP-NARX						OI GP uncertainty			
Aim #2				Proposed approach		Generalization + bifurcations						
Aim #3				Proposed approach		Algorithm						
Aim #4			DMA-MR (2x2)									
			NGCC (2x2, 8x3)				CSTR-AD, DMA-AD		Depropanizer			
Journal Publications			CACE – GP [47]				AIChE Journal – Inverse mapping with AD [48]					
							Implicit mapping generalization					
									ArXiv - Python tool			
							Control structure OI					
Defense							Dissertation					

Figure 12: Research Timeline.

References

- [1] F. V. Lima and C. Georgakis, "Input–output operability of control systems: The steady-state case," *Journal of Process Control*, vol. 20, no. 6, pp. 769–776, 2010, ISSN: 0959-1524. DOI: <https://doi.org/10.1016/j.jprocont.2010.04.008>.
- [2] V. Gazzaneo, J. C. Carrasco, D. R. Vinson, and F. V. Lima, "Process operability algorithms: Past, present, and future developments," *Industrial & Engineering Chemistry Research*, vol. 59, no. 6, pp. 2457–2470, 2020. DOI: 10.1021/acs.iecr.9b05181. eprint: <https://doi.org/10.1021/acs.iecr.9b05181>.
- [3] D. R. Vinson and C. Georgakis, "A new measure of process output controllability," *Journal of Process Control*, vol. 10, no. 2, pp. 185 –194, 2000, ISSN: 0959-1524. DOI: [https://doi.org/10.1016/S0959-1524\(99\)00045-1](https://doi.org/10.1016/S0959-1524(99)00045-1).
- [4] C. Georgakis, D. Uztürk, S. Subramanian, and D. R. Vinson, "On the operability of continuous processes," *Control Engineering Practice*, vol. 11, no. 8, pp. 859 –869, 2003, Process Dynamics and Control, ISSN: 0967-0661. DOI: [https://doi.org/10.1016/S0967-0661\(02\)00217-4](https://doi.org/10.1016/S0967-0661(02)00217-4).
- [5] C. Georgakis and L. Li, "On the calculation of operability sets of nonlinear high-dimensional processes," *Industrial & Engineering Chemistry Research*, vol. 49, no. 17, pp. 8035–8047, 2010. DOI: 10.1021/ie1009316. eprint: <https://doi.org/10.1021/ie1009316>.
- [6] S. Subramanian and C. Georgakis, "Methodology for the steady-state operability analysis of plantwide systems," *Industrial & Engineering Chemistry Research*, vol. 44, no. 20, pp. 7770–7786, 2005. DOI: 10.1021/ie0490076. eprint: <https://doi.org/10.1021/ie0490076>.
- [7] J. C. Carrasco and F. V. Lima, "Nonlinear operability of a membrane reactor for direct methane aromatization," *IFAC-PapersOnLine*, vol. 48, no. 8, pp. 728 –733, 2015, 9th IFAC Symposium on Advanced Control of Chemical Processes ADCHEM 2015, ISSN: 2405-8963. DOI: <https://doi.org/10.1016/j.ifacol.2015.09.055>.
- [8] J. C. Carrasco and F. V. Lima, "Novel operability-based approach for process design and intensification: Application to a membrane reactor for direct methane aromatization," *AICHE Journal*, vol. 63, no. 3, pp. 975–983, 2017. DOI: <https://doi.org/10.1002/aic.15439>. eprint: <https://aiche.onlinelibrary.wiley.com/doi/pdf/10.1002/aic.15439>.
- [9] J. C. Carrasco and F. V. Lima, "An optimization-based operability framework for process design and intensification of modular natural gas utilization systems," *Computers & Chemical Engineering*, vol. 105, pp. 246 –258, 2017, ISSN: 0098-1354. DOI: <https://doi.org/10.1016/j.compchemeng.2016.12.010>.
- [10] V. Gazzaneo and F. V. Lima, "Multilayer operability framework for process design, intensification, and modularization of nonlinear energy systems," *Industrial & Engineering Chemistry Research*, vol. 58, no. 15, pp. 6069–6079, 2019. DOI: 10.1021/acs.iecr.8b05482. eprint: <https://doi.org/10.1021/acs.iecr.8b05482>.
- [11] J. C. Carrasco and F. V. Lima, "Bilevel and parallel programming-based operability approaches for process intensification and modularity," *AICHE Journal*, vol. 64, no. 8, pp. 3042–3054, 2018. DOI: <https://doi.org/10.1002/aic.16113>. eprint: <https://aiche.onlinelibrary.wiley.com/doi/pdf/10.1002/aic.16113>.
- [12] J. Hadamard, "Sur les problèmes aux dérivées partielles et leur signification physique," *Princeton University Bulletin*, vol. 13, pp. 49–52, 1902.
- [13] A. Tikhonov, A. Goncharsky, V. Stepanov, and A. Yagola, *Numerical Methods for the Solution of Ill-Posed Problems* (Mathematics and Its Applications). Springer Netherlands, 1995, ISBN: 9780792335832.
- [14] V. Gazzaneo, J. C. Carrasco, and F. V. Lima, "An MILP-based operability approach for process intensification and design of modular energy systems," in *13th International Symposium on Process Systems Engineering (PSE 2018)*, ser. Computer Aided Chemical Engineering, M. R. Eden, M. G. Ierapetritou, and G. P. Towler, Eds., vol. 44, Elsevier, 2018, pp. 2371–2376. DOI: <https://doi.org/10.1016/B978-0-444-64241-7.50390-6>.
- [15] R. C. Aster, B. Borchers, and C. H. Thurber, *Parameter estimation and inverse problems*, English, Amsterdam ; 2018. DOI: 10.1016/C2015-0-02458-3.
- [16] D. O. Baguer, J. Leuschner, and M. Schmidt, "Computed tomography reconstruction using deep image prior and learned reconstruction methods," *Inverse Problems*, vol. 36, no. 9, p. 094004, 2020. DOI: 10.1088/1361-6420/aba415.

- [17] K. Akiyama, A. Alberdi, W. Alef, K. Asada, R. Azulay, A.-K. Baczko, D. Ball, M. Baloković, J. Barrett, D. Bintley, *et al.*, “First m87 event horizon telescope results. iv. imaging the central supermassive black hole,” *The Astrophysical Journal Letters*, vol. 875, no. 1, p. L4, 2019.
- [18] W. Daosud, P. Thitiyasook, A. Arpornwichanop, P. Kittisupakorn, and M. A. Hussain, “Neural network inverse model-based controller for the control of a steel pickling process,” *Computers & Chemical Engineering*, vol. 29, no. 10, pp. 2110–2119, 2005, ISSN: 0098-1354. DOI: <https://doi.org/10.1016/j.compchemeng.2005.06.007>.
- [19] M. Sharifzadeh and N. F. Thornhill, “Integrated design and control using a dynamic inversely controlled process model,” *Computers & Chemical Engineering*, vol. 48, pp. 121–134, 2013.
- [20] F. Ceccon, J. Jalving, J. Haddad, A. Thebelt, C. Tsay, C. D. Laird, and R. Misener, *OmLt: Optimization & machine learning toolkit*, 2022. arXiv: 2202.02414 [stat.ML].
- [21] L. M. Umar, W. Hu, Y. Cao, and V. Kariwala, “Selection of controlled variables using self-optimizing control method,” in *Plantwide Control*. John Wiley & Sons, Ltd, 2012, ch. 4, pp. 43–71, ISBN: 9781119968962. DOI: <https://doi.org/10.1002/9781119968962.ch4>. eprint: <https://onlinelibrary.wiley.com/doi/pdf/10.1002/9781119968962.ch4>.
- [22] S. Skogestad, “Plantwide control: The search for the self-optimizing control structure,” *Journal of Process Control*, vol. 10, no. 5, pp. 487–507, 2000, ISSN: 0959-1524. DOI: [https://doi.org/10.1016/S0959-1524\(00\)00023-8](https://doi.org/10.1016/S0959-1524(00)00023-8).
- [23] A. C. de Araújo, M. Govatsmark, and S. Skogestad, “Application of plantwide control to the hda process. i—steady-state optimization and self-optimizing control,” *Control Engineering Practice*, vol. 15, no. 10, pp. 1222 –1237, 2007, Special Issue - International Symposium on Advanced Control of Chemical Processes (ADCHEM), ISSN: 0967-0661. DOI: <https://doi.org/10.1016/j.conengprac.2006.10.014>.
- [24] A. Araújo and S. Skogestad, “Control structure design for the ammonia synthesis process,” *Computers & Chemical Engineering*, vol. 32, no. 12, pp. 2920–2932, 2008, ISSN: 0098-1354. DOI: <https://doi.org/10.1016/j.compchemeng.2008.03.001>.
- [25] Y. Cao, D. Rossiter, and D. H. Owens, “Globally optimal control structure selection using branch and bound method,” *IFAC Proceedings Volumes*, vol. 31, no. 11, pp. 185 –190, 1998, 5th IFAC Symposium on Dynamics and Control of Process Systems 1998 (DYCOPS 5), Corfu, Greece, 8-10 June 1998, ISSN: 1474-6670. DOI: [https://doi.org/10.1016/S1474-6670\(17\)44926-3](https://doi.org/10.1016/S1474-6670(17)44926-3).
- [26] Y. Cao and P. Saha, “Improved branch and bound method for control structure screening,” *Chemical Engineering Science*, vol. 60, no. 6, pp. 1555 –1564, 2005, ISSN: 0009-2509. DOI: <https://doi.org/10.1016/j.ces.2004.10.025>.
- [27] P. Saha and Y. Cao, “Globally optimal control structure selection using hankel singular value through branch and bound method,” in *Process Systems Engineering 2003, 8th International Symposium on Process Systems Engineering*, ser. Computer Aided Chemical Engineering, B. Chen and A. W. Westerberg, Eds., vol. 15, Elsevier, 2003, pp. 1014 –1019. DOI: [https://doi.org/10.1016/S1570-7946\(03\)80441-8](https://doi.org/10.1016/S1570-7946(03)80441-8).
- [28] V. Kariwala, Y. Cao, and S. Janardhanan, “Local self-optimizing control with average loss minimization,” *Industrial & Engineering Chemistry Research*, vol. 47, no. 4, pp. 1150–1158, 2008. DOI: [10.1021/ie070897+](https://doi.org/10.1021/ie070897+). eprint: <https://doi.org/10.1021/ie070897+>.
- [29] V. Kariwala and Y. Cao, “Bidirectional branch and bound for controlled variable selection. part ii: Exact local method for self-optimizing control,” *Computers & chemical engineering*, vol. 33, no. 8, pp. 1402–1412, 2009.
- [30] F. V. Lima, Z. Jia, M. Ierapetritou, and C. Georgakis, “Similarities and differences between the concepts of operability and flexibility: The steady-state case,” *AIChE Journal*, vol. 56, no. 3, pp. 702–716, 2010. DOI: <https://doi.org/10.1002/aic.12021>.
- [31] S. Lophaven, H. Nielsen, and J. Søndergaard, *DACE - A Matlab Kriging Toolbox, Version 2.0*, English. 2002.
- [32] S. N. Lophaven, H. B. Nielsen, and J. Søndergaard, “Aspects of the matlab toolbox DACE,” Informatics and Mathematical Modelling, Technical University of Denmark, DTU, Richard Petersens Plads, Building 321, DK-2800 Kgs. Lyngby, Tech. Rep., 2002.

- [33] J. A. Caballero and I. E. Grossmann, “An algorithm for the use of surrogate models in modular flowsheet optimization,” *AICHE Journal*, vol. 54, no. 10, pp. 2633–2650, 2008. doi: 10.1002/aic.11579. eprint: <https://aiche.onlinelibrary.wiley.com/doi/pdf/10.1002/aic.11579>.
- [34] N. Quirante, J. Javaloyes, R. Ruiz-Femenia, and J. A. Caballero, “Optimization of chemical processes using surrogate models based on a kriging interpolation,” in *12th International Symposium on Process Systems Engineering and 25th European Symposium on Computer Aided Process Engineering*, ser. Computer Aided Chemical Engineering, K. V. Gernaey, J. K. Huusom, and R. Gani, Eds., vol. 37, Elsevier, 2015, pp. 179–184. doi: <https://doi.org/10.1016/B978-0-444-63578-5.50025-6>.
- [35] J. Sacks, W. J. Welch, T. J. Mitchell, and H. P. Wynn, “Design and analysis of computer experiments,” *Statistical science*, pp. 409–423, 1989.
- [36] A. Forrester, A. Sobester, and A. Keane, *Engineering design via surrogate modelling: a practical guide*. John Wiley & Sons, 2008.
- [37] C. E. Rasmussen and H. Nickisch, “Gaussian processes for machine learning (gpml) toolbox,” *Journal of machine learning research*, vol. 11, no. Nov, pp. 3011–3015, 2010.
- [38] D. R. Jones, “A taxonomy of global optimization methods based on response surfaces,” *Journal of global optimization*, vol. 21, no. 4, pp. 345–383, 2001.
- [39] C. E. Rasmussen and C. K. I. Williams, *Gaussian processes for machine learning*. MIT Press, 2008.
- [40] V. M. C. Alves, F. S. Lima, S. K. Silva, and A. C. B. Araujo, “Metamodel-based numerical techniques for self-optimizing control,” *Industrial & Engineering Chemistry Research*, vol. 57, no. 49, pp. 16817–16840, 2018. doi: 10.1021/acs.iecr.8b04337. eprint: <https://doi.org/10.1021/acs.iecr.8b04337>.
- [41] F. S. Lima, V. M. C. Alves, and A. C. B. de Araujo, “Metacontrol: A python based application for self-optimizing control using metamodels,” *Computers & Chemical Engineering*, vol. 140, p. 106979, 2020, ISSN: 0098-1354. doi: <https://doi.org/10.1016/j.compchemeng.2020.106979>.
- [42] M. van de Wal and B. de Jager, “A review of methods for input/output selection,” *Automatica*, vol. 37, no. 4, pp. 487–510, 2001, ISSN: 0005-1098. doi: [https://doi.org/10.1016/S0005-1098\(00\)00181-3](https://doi.org/10.1016/S0005-1098(00)00181-3).
- [43] S. Vasudevan and G. P. Rangaiah, “A review of plantwide control methodologies and applications,” in *Plantwide Control*. John Wiley & Sons, Ltd, 2012, ch. 9, pp. 179–201, ISBN: 9781119968962. doi: <https://doi.org/10.1002/9781119968962.ch9>. eprint: <https://onlinelibrary.wiley.com/doi/pdf/10.1002/9781119968962.ch9>.
- [44] Y. Cao and V. Kariwala, “Bidirectional branch and bound for controlled variable selection: Part i. principles and minimum singular value criterion,” *Computers & Chemical Engineering*, vol. 32, no. 10, pp. 2306–2319, 2008, ISSN: 0098-1354. doi: <https://doi.org/10.1016/j.compchemeng.2007.11.011>.
- [45] D. Jones, D. Bhattacharyya, R. Turton, and S. E. Zitney, “Plant-wide control system design: Primary controlled variable selection,” *Computers & Chemical Engineering*, vol. 71, pp. 220–234, 2014, ISSN: 0098-1354. doi: <https://doi.org/10.1016/j.compchemeng.2014.08.004>.
- [46] D. R. Vinson and C. Georgakis, “Inventory control structure independence of the process operability index,” *Industrial & Engineering Chemistry Research*, vol. 41, no. 16, pp. 3970–3983, 2002. doi: 10.1021/ie0109814. eprint: <https://doi.org/10.1021/ie0109814>.
- [47] V. Alves, V. Gazzaneo, and F. V. Lima, “A machine learning-based process operability framework using gaussian processes,” *Computers & Chemical Engineering*, vol. 163, p. 107835, 2022, ISSN: 0098-1354. doi: <https://doi.org/10.1016/j.compchemeng.2022.107835>.
- [48] V. Alves, J. R. Kitchin, and F. V. Lima, “An inverse mapping approach for process systems engineering using automatic differentiation and the implicit function theorem,” *AICHE Journal*, vol. n/a, no. n/a, e18119, DOI: <https://doi.org/10.1002/aic.18119>. eprint: <https://aiche.onlinelibrary.wiley.com/doi/pdf/10.1002/aic.18119>.
- [49] J. Bradbury, R. Frostig, P. Hawkins, M. J. Johnson, C. Leary, D. Maclaurin, G. Necula, A. Paszke, J. VanderPlas, S. Wanderman-Milne, and Q. Zhang, *JAX: Composable transformations of Python+NumPy programs*, version 0.3.13, 2018.

- [50] H. Keller, “Numerical solution of bifurcation and nonlinear eigenvalue problem,” *Application of Bifurcation Theory*, 1977.
- [51] T. F. C. Chan and H. B. Keller, “Arc-length continuation and multigrid techniques for nonlinear elliptic eigenvalue problems,” *SIAM Journal on Scientific and Statistical Computing*, vol. 3, no. 2, pp. 173–194, 1982. DOI: 10.1137/0903012. eprint: <https://doi.org/10.1137/0903012>.
- [52] S. M. Cavalcanti and P. I. Barton, “Multiple steady states and nonsmooth bifurcations in dry and vaporless distillation columns,” *Industrial & Engineering Chemistry Research*, vol. 59, no. 40, pp. 18 000–18 018, 2020. DOI: 10.1021/acs.iecr.0c02328. eprint: <https://doi.org/10.1021/acs.iecr.0c02328>.
- [53] U. A. Al-Mubaiyedh and H. Binous, “Teaching arc-length continuation in the chemical engineering graduate program using matlab[®],” *Computer Applications in Engineering Education*, vol. 26, no. 4, pp. 1033–1049, 2018. DOI: <https://doi.org/10.1002/cae.21954>. eprint: <https://onlinelibrary.wiley.com/doi/pdf/10.1002/cae.21954>.
- [54] W. L. Luyben, “Evaluation of criteria for selecting temperature control trays in distillation columns,” *Journal of Process Control*, vol. 16, no. 2, pp. 115–134, 2006, ISSN: 0959-1524. DOI: <https://doi.org/10.1016/j.jprocont.2005.05.004>.
- [55] E. Hori and S. Skogestad, “Selection of control structure and temperature location for two-product distillation columns,” *Chemical Engineering Research and Design*, vol. 85, no. 3, pp. 293–306, 2007, ISSN: 0263-8762. DOI: <https://doi.org/10.1205/cherd06115>.
- [56] S. Dinh and F. V. Lima, “Dynamic operability analysis for process design and control of modular natural gas utilization systems,” *Industrial & Engineering Chemistry Research*, vol. 62, no. 5, pp. 2052–2066, 2023. DOI: 10.1021/acs.iecr.2c03543. eprint: <https://doi.org/10.1021/acs.iecr.2c03543>.
- [57] J. Kocijan, *Modelling and Control of Dynamic Systems Using Gaussian Process Models* (Advances in Industrial Control). Springer International Publishing, 2015, ISBN: 9783319210216.
- [58] W. L. Luyben, “Design and control of the ethyl benzene process,” *AICHE Journal*, vol. 57, no. 3, pp. 655–670, 2011. DOI: <https://doi.org/10.1002/aic.12289>. eprint: <https://aiche.onlinelibrary.wiley.com/doi/pdf/10.1002/aic.12289>.
- [59] V. Gazzaneo, M. Watson, C. B. Ramsayer, Z. A. Kilwein, V. Alves, and F. V. Lima, “A techno-economic analysis framework for intensified modular systems,” *Journal of Advanced Manufacturing and Processing*, vol. 4, no. 3, e10115, 2022. DOI: <https://doi.org/10.1002/amp2.10115>. eprint: <https://aiche.onlinelibrary.wiley.com/doi/pdf/10.1002/amp2.10115>.